

The Effect of Shock-Wave Parameters  
on the Strengthening of Nickel and Iron

R. N. Orava, M. A. Meyers, and G. A. Stone  
Department of Metallurgical Engineering  
South Dakota School of Mines and Technology  
Rapid City, S.D. 57701, U.S.A.

Abstract

A study was conducted to evaluate the effect of shock-wave profile on the hardening and microstructural response of unalloyed, polycrystalline nickel and iron. The peak pressure, peak pressure duration, and rarefaction rate were varied independently by appropriately controlling the material or thickness of the driver plate, and amount of explosive, used in parallel-plate or inclined plate plane-wave generators. Shock pressures ranged from 8 to 35 GPa, pressure durations from 0.5 to 2.0  $\mu$ s, and rarefaction rates from -30 to -100 GPa/ $\mu$ s.

In nickel, it was found that the hardness and dislocation cell size was a function of all three parameters. In iron, the hardness and deformation structure was observed to vary with pressure and pressure duration but not with rarefaction rate in a systematic way. A mechanistic interpretation of these findings is presented.

1. Introduction

At the Vth International Conference on High Energy Rate Fabrication, Orava and Wittman<sup>1</sup> detailed techniques for the independent variation of three shock-wave parameters during plate-impact experiments. These parameters are: peak pressure ( $P_m$ ); duration of peak pressure ( $t_p$ ); and the rarefaction rate ( $\dot{P}_p$ ) representing the rate at which the pressure is released at the tail of a "square" shock pulse. In summary, the peak pressure can be varied in plane-wave impact loading by changing the driver-plate velocity. In order to maintain a constant pulse duration, however, the thickness of the driver plate must be adjusted accordingly. In order, further, to maintain a constant rarefaction rate, it was deduced that the driver plate must also be changed appropriately. Therefore, one is limited to the selection of shock pressures which are discrete, not forming a continuous spectrum. This selection procedure has been computerized according to materials which are readily available and whose Hugoniot characteristics have been determined.

The phenomenon of shock hardening of metals and alloys is well known, with residual strength increasing with increasing shock pressure until in-situ thermal recovery efforts become a factor at higher shock pressures. Moreover, considerable recent evidence in the literature also points to the fact that substructure and strength can be influenced by changing the duration of the peak pressure when the peak pressure is kept at a constant value. This information has been reviewed by Meyers in a recent publication<sup>2</sup>. He considered the results of experiments on copper<sup>3</sup>, Hadfield steel<sup>4</sup>, nickel<sup>5</sup>, Inconel 600 (76% Ni, 16% Cr, 7% Fe)<sup>6</sup>, Chromel A (80% Ni - 20% Cr)<sup>7</sup>, AISI 304 stainless

steel<sup>7</sup>, and Cu - 8.7% Ge<sup>8</sup>. The most common trend was for the hardness<sup>3-5, 8</sup> and strength<sup>6</sup> to increase as the pressure duration was increased, accompanied by a refinement in the dislocation substructure<sup>3</sup> and increase in dislocation density<sup>5</sup>. However, the extent of the effect appeared to be a function of the magnitude of both the pressure and the duration. Moreover, in the case of nickel<sup>5</sup> no change in hardness resulted when duration was increased from 1 to 2  $\mu$ s at 25 GPa, and for 304 stainless steel<sup>7</sup>, the same conditions led to a hardness decrease. Nevertheless, in reviewing these data, Meyers<sup>2</sup> concluded that pulse duration is a factor which, when varied appropriately, can produce changes of the same order of magnitude as varying peak pressure.

Appleton and Waddington<sup>3</sup> first expressed concern that some of the duration effect which they observed might have been the consequence of the influence of an uncontrollable change in the rarefaction rate. They were unable to satisfactorily resolve this problem. Champion and Rohde<sup>4</sup> utilized different shock-loading techniques in an effort to circumvent this difficulty. Heretofore, no work has been done on evaluating what influence rarefaction rate itself might have on the response to shock loading. The procedure<sup>1</sup> for independently varying the three shock-wave parameters in plate-impact experiments was devised in an attempt to generate such information. In addition, it would serve to determine whether an inadvertent variation in rarefaction rate might have influenced the results of previous studies of pressure and duration dependence.

In this conference paper, the authors provide some experimental data on unalloyed nickel and iron which were shock loaded by successively maintaining constant two of the three parameters --  $P_m$ ,  $t_p$ , and  $P_R$ .

## 2. Experiment Procedures

### 2.1 Materials

The materials studied were Nickel 270 (>99.98 wt. pct. purity) and Armco Magnetic Ingot Iron (0.006% C, 0.006% N, and 0.004% O, by weight), hereinafter identified as nickel and iron. The nickel sheet, 3 mm. in thickness, was annealed at 700°C for one hour in an argon atmosphere, yielding an average grain diameter of 0.100 mm. The iron, also in sheet form of thickness 3 mm, was annealed at 730°C for one-half hour in an argon atmosphere, resulting in an average grain diameter of 0.130 mm. All heat treatments were performed after cutting samples to 7.6 cm by 10.2 cm plates in order to remove all cold work due to machining.

### 2.2 Shock-Loading Procedure

Shock deformation was achieved by utilizing either an inclined-plate or parallel-plate plane-wave generator of the type illustrated previously<sup>1</sup>. DuPont Deta Sheet "C" PETN-based plastic explosive was used as the line-wave generator and main charge for all shots. For Detasheet "C", Gurney characteristic velocities of 2240 m/s and 2970 m/s were used for the inclined-plate and parallel-plate shots, respectively.

The nickel and iron specimens were shocked separately but the geometry of the specimen assemblies, shown schematically in Figure 1, was virtually identical for both materials. Two specimens, with the highest purity material

nearest the incident surface, were sandwiched between a protective cover plate and spall plate, and surrounded by momentum or spall rails. The whole assembly was then placed on an anvil plate. For shock loading nickel, all spall materials were nickel-based alloys with a high nickel content. For shock loading iron, all spall materials were plain, low-carbon steels. The specimen assemblies were propelled into water by driver-plate impact, in order to minimize residual thermal effects.

The shock-loading conditions for nickel are listed in Table 1 and for iron, in Table 2.

### 3. Results and Discussion

#### 3.1 Nickel

The effect of the profile of a plane shock wave on the residual hardness (DPH, 0.1 kg load) of nickel is recorded in Table 3. The data are subdivided into three categories: (a) variable pressure, constant duration and rarefaction rate; (b) variable duration, constant pressure and rarefaction rate; and (c) variable rarefaction rate, constant pressure and duration.

Consistent with previous work on shock-loaded nickel, when the shock pressure is increased to 35 GPa, the hardness increases. However, the shock-hardening rate appears to depend somewhat on the magnitude of the duration and rarefaction rate, as illustrated in Figure 2. A 2- $\mu$ s pulse yields a lower work-hardening rate than a 1- $\mu$ s pulse when the rarefaction rate is approximately constant at -63 GPa/ $\mu$ s. A more rapid pressure release is responsible for a still lower rate of hardening when the pulse duration is 1- $\mu$ s in both cases.

Figure 2 also provides a comparison with the results of previous investigations. The shock-hardening curves obtained by Dieter<sup>9</sup> and by Nolder and Thomas<sup>10</sup> exhibit inflections in the 20 and 30 GPa pressure range. Murr et al<sup>11</sup> also found a sharp rise in hardness at about 20 GPa. If one were to join the 2- $\mu$ s data point at 9.4 GPa to the 1- $\mu$ s data point at 35 GPa (both at  $\dot{P}_R$  = -63 GPa/ $\mu$ s), then a departure from a continuously decreasing slope might be obtained. A similar exercise, at a constant duration of 1  $\mu$ s, joining the point at 9.4 GPa,  $\dot{P}_R$  = -95 GPa/ $\mu$ s, with that at 35 GPa,  $\dot{P}_R$  = -63 GPa/ $\mu$ s, could also lead to an apparent inflection in the curve. It is worth noting that the pulse duration in Dieter's experiments<sup>9</sup> changed from 2  $\mu$ s to 1  $\mu$ s in going from a pressure of 26.5 GPa to 36 GPa. Neither Trueb<sup>12</sup> nor Rose et al<sup>13</sup> reported any inflections in their shock-hardening curves. The results of Rose et al<sup>13</sup> fell directly on the 1  $\mu$ s, -63 GPa/ $\mu$ s hardening curve from the current study.

It is postulated that those shock-hardening curves for nickel which exhibit changes in the sign of the second derivative reflect the fact that either duration and/or rarefaction rate changed significantly when pressure was varied.

Transmission electron microscopy revealed that dislocation cell sizes, also listed in Table 3, were in good agreement with hardness values; smaller cell diameters at the higher pressure corresponded to harder material. Typical substructures for Ni 270 shocked at 9.4 and 35 GPa are shown in

Table 1. Explosive Loading Conditions for Nickel

<u>Driver Material</u>	<u>Driver Thickness (mm)</u>	<u>Peak Pressure (GPa)</u>	<u>Pressure Duration (<math>\mu</math>s)</u>	<u>Average Rarefaction Rate (GPa/<math>\mu</math>s)</u>
Ni	5.12	9.4	2.0	-55.8
Al	3.29	9.4	1.0	-56.5
Ni	2.58	9.4	1.0	-93.1
Cu	2.82	35.0	1.0	-98.2
Ni	6.29	35.0	2.0	-69.4
1018 Steel	3.16	35.0	1.0	-68.7
1018 Steel	6.16	35.0	2.0	-38.1

Table 2. Explosive Loading Conditions for Iron

<u>Driver Material</u>	<u>Driver Thickness (mm)</u>	<u>Peak Pressure (GPa)</u>	<u>Pressure Duration (<math>\mu</math>s)</u>	<u>Average Rarefaction Rate (GPa/<math>\mu</math>s)</u>
Ni	2.67	8.0	1.0	-51.6
1018 Steel	1.93	8.0	1.0	-34.9
304 SS	4.97	8.0	2.0	-35.0
304 SS	2.79	10.0	1.0	-51.4
1018 Steel	2.53	10.0	1.0	-36.5
304 SS	5.03	10.0	2.0	-36.4
Cu	2.58	13.0	1.0	-51.0
1018 Steel	2.28	13.0	1.0	-38.8
304 SS	5.44	13.0	2.0	-38.5
2024 Al	1.93	18.0	0.5	-63.8
Ni	2.77	18.0	1.0	-63.3
1018 Steel	2.69	18.0	1.0	-42.5
2024 Al	2.11	25.0	0.5	-71.8
Ni	3.03	25.0	1.0	-70.5
2024 Al	4.21	25.0	1.0	-51.1
921T Al	2.52	35.0	0.5	-78.0
Ni	3.36	35.0	1.0	-79.9
1018 Steel	3.29	35.0	1.0	-53.3

Table 3. Hardness Data and Dislocation Cell Sizes for Shock-Loaded Ni 270

<u>Peak Pressure (GPa)</u>	<u>Pressure Duration (<math>\mu</math>s)</u>	<u>Rarefaction Rate (GPa/<math>\mu</math>s)</u>	<u>Hardness (DPH)</u>	<u>Dislocation Cell Size (<math>\mu</math>m)</u>
<u>(a) PRESSURE VARIABLE</u>				
94	1	-56.5	155	0.51
350	1	-68.7	196	0.39
94	1	-93.1	141	0.58
350	1	-98.2	175	0.48
94	2	-55.8	149	0.69
350	2	-69.4	181	0.41
<u>(b) DURATION VARIABLE</u>				
94	1	-56.5	155	0.51
94	2	-55.8	149	0.69
350	1	-68.7	196	0.39
350	2	-69.4	181	0.41
<u>(c) RAREFACTION RATE VARIABLE</u>				
94	1	-56.5	155	0.51
94	1	-93.1	141	0.58
350	1	-68.7	196	0.39
350	1	-98.2	175	0.48
350	2	-38.1	182	0.29
350	2	-69.4	181	0.41

Figures 3(a) and 3(b), clearly delineating the reason for the pressure dependence of hardening.

A change in pulse duration from 1  $\mu$ s to 2  $\mu$ s, at constant pressure and rarefaction rate, results in an increase in the cell size in nickel with a corresponding reduction in residual hardness (Table 3). However, the effect is not as pronounced as that which accompanies the pressure increase from 9.4 to 35 GPa as seen when Figures 3(a) and 3(c) are compared. The above behavior is not inconsistent with that found by Murr and Huang<sup>6</sup> and confirmed recently by Murr and Kuhlmann-Wilsdorf<sup>14</sup> on re-examination of the specimens used by Murr and Huang<sup>6</sup> and other investigators. Murr and Kuhlmann-Wilsdorf<sup>14</sup> concluded that the dislocation cell size and dislocation density are approximately constant between 1 and 6  $\mu$ s at 25 GPa and that the hardening saturates over the same range. If anything, in their work, the cells tended to be smaller as duration was increased, whereas Table 3 indicates the reverse trend. When driver-plate thickness is increased in order to increase duration at a constant pressure, there exists the potential for a large decrease in rarefaction rate. Since, according to Table 3, this in itself will lead to a smaller cell size with increasing duration, it is the present authors' contention that an increase in duration can produce larger cells in nickel if rarefaction rate is kept constant but smaller cells if rarefaction rate is not controlled.

The increase in cell size with increased pulse duration can be attributed to the increase in time available for cell growth and dislocation annihilation at pressure, in the presence of a relatively high, transient temperature.

When rarefaction rate only is the dependent variable, the data in Table 3 reveal that hardness tends to be lower and cell size larger when the rarefaction rate is increased. The electron micrographs in Figures 3(b) and 3(d) demonstrate visually that the cell sizes can be different for different rates of pressure release.

For the interpretation of the rarefaction-rate dependence of the substructure, one must assume--for conditions of constant pressure and rarefaction rate--that the dislocation cell size is the same for all rarefaction rates just at the point where pressure release begins. In addition, the results are consistent with the view that further substructure refinement can occur during the rarefaction phase of the shock pulse. This behavior is understandable when one considers that an effective reversal in loading will lead to dislocations moving back into cell interiors and interacting therein to become entangled to form new cell walls. Moreover, the data indicate that the lower the rate of release of pressure, the finer is the substructure. Since higher stresses operate for a longer period of time when the pressure is released more gradually, more dislocations can be generated from appropriate sources. In turn, these dislocations can move shorter distances to accommodate the strain. The net result is a small dislocation cell size.

### 3.2 Iron

The effect of peak pressure on the shock-hardening response of iron at a constant duration of 1  $\mu$ s and rarefaction rate of -52 GPa/ $\mu$ s is shown in Figure 4. The sudden increase in residual hardness beyond 13 GPa, the transition pressure, is evident. However, when the results are compared with those of Zukas<sup>15</sup>, which they closely parallel, and those of Dieter<sup>16</sup>, the range over which the sharp rise in hardness occurs is displaced about 5 GPa toward higher

pressures. Neither Zukas nor Dieter made any attempt to control parameters other than peak pressure.

Optical metallography revealed the traditionally observed increase in the percentage of grains which contained twin-like markings and the volume fraction of such markings within those grains when pressure is increased. These data, converted to the volume fraction of deformation markings and plotted against peak pressure in Figure 5, indicate overall agreement with the hardening curve in Figure 4. Although x-ray diffraction analysis revealed only the presence of  $\alpha$ -phase (BCC) in all shocked specimens, the authors are not prepared to identify the observed markings as twins until transmission electron microscopy has been carried out.

When the pressure duration is changed at constant pressure and rarefaction rate, the data in Table 4 disclose that duration becomes an important variable, for the durations examined, in the region where two plastic waves exist, i.e. 13 to 33 GPa, reflected by the results for 18 and 25 GPa shock pressures. The density of deformation markings (Figure 5) exhibit behavior consistent with the hardness data for 0.5  $\mu$ s and -70 GPa/ $\mu$ s in Figure 4.

These results are thought to be a manifestation of the retardation of the nucleation of the  $\epsilon$ -phase until the peak pressure reaches some critical value for a given duration, in this case 0.5  $\mu$ s. Figure 6 shows the microstructures for iron shocked at 25 GPa and -71 GPa/ $\mu$ s but at different durations.

It is interesting that Staudhammer and Murr<sup>17</sup> observed, for stainless steel, increasing amounts of martensite and twins with increasing pulse durations. Similar results were found by Meyers<sup>18</sup>: the amount of a martensite, as determined by attraction of shocked samples to a magnet, increased substantially for pulse durations of 1.2, 2.4, and 10.1  $\mu$ sec, at a pressure of 20 GPa.

The results for the variation only in rarefaction rate are presented in Table 5. The dependence of residual hardness and microstructure on rarefaction is neither extensive nor systematic for the loading conditions applied. The largest difference in hardness and deformation structure occurred for iron shock loaded at 18 GPa, where the higher rarefaction rate led to a higher hardness and higher density of deformation markings. On shock loading to 35 GPa, the higher rarefaction rate also produced a higher density of observably finer deformation markings.

While these results might be understandable in terms of the necessity to accommodate strains during the reverse transformation from  $\epsilon$  to  $\alpha$  in a shorter pressure release period, the inconsistency of the behavior suggests that there is probably a balance among several products of the shock deformation--dislocations, mechanical twins generated by deformation only, and those twins or dislocations produced by the phase transformation.

#### 4. Summary and Conclusions

The major observations and the conclusions which can be drawn therefrom can be summarized as follows:



Table 4. Effect of Pulse Duration on the Hardness and Deformation Markings in Magnetic Ingot Iron.

Pressure Duration ( $\mu$ s)	Peak Pressure (GPa)	Rarefaction Rate (GPa/ $\mu$ s)	Hardness (DPH)	Volume Fraction of Deformation Markings
1.0	8.0	-34.9	116	0.006
2.0	8.0	-35.0	109	0.003
1.0	10.0	-36.5	125	0.08
2.0	10.0	-36.4	122	0.09
1.0	13.0	-38.8	145	0.12
2.0	13.0	-38.5	120	0.11
0.5	18.0	-63.8	125	0.04
1.0	18.0	-63.3	195	0.46
0.5	25.0	-71.8	119	0.01
1.0	25.0	-70.5	230	0.29
0.5	35.0	-78.0	239	0.62
1.0	35.0	-79.9	237	0.73

Table 5. Effect of Rarefaction Rate on the Hardness and Deformation Markings in Magnetic Ingot Iron.

Rarefaction Rate (GPa/ $\mu$ s)	Peak Pressure (GPa)	Pressure Duration ( $\mu$ s)	Hardness (DPH)	Volume Fraction of Deformation Markings
-51.6	8.0	1.0	109	0
-34.9	8.0	1.0	116	0.01
-51.4	10.0	1.0	120	0.002
-36.5	10.0	1.0	125	0.08
-51.0	13.0	1.0	130	0.08
-38.8	13.0	1.0	145	0.12
-63.3	18.0	1.0	195	0.46
-42.5	18.0	1.0	159	0.07
-70.5	25.0	1.0	230	0.29
-51.1	25.0	1.0	242	0.35
-79.9	35.0	1.0	237	0.73
-53.3	35.0	1.0	214	0.52

1. When the pressure duration and rarefaction rate are held constant, the curve of hardness versus shock pressure for nickel has a continuously decreasing slope, at least up to 35 GPa. Inflections observed previously are believed to be due to variations in pressure duration and rarefaction rate.
2. When pressure and rarefaction rate are held constant, an increase in pressure duration from 1 to 2  $\mu$ s will result in a small but consistent decrease in the hardness and increase in dislocation cell size of nickel. This behavior was attributed to the longer time available for cell growth and dislocation rearrangement under stress at an elevated, transient temperature.
3. When pressure and duration are held constant, nickel exhibits an increase in hardness and decrease in dislocation cell size with decreasing rarefaction rate. ~~The authors ascribe this trend to~~ <sup>ascribed</sup> the greater refinement of the shock-generated substructure when the pressure is released more slowly.
4. The shock pressure dependence of the residual hardness of iron is consistent with previous findings, with the exception that the sharp rise in hardness resulting from the pressure transition at 13 GPa appears to be shifted to a higher pressure when duration and rarefaction rate are controlled.
5. When iron is shock loaded, a reduction in pressure duration to 0.5  $\mu$ s further shifts, by approximately 20 GPa, to 33 GPa, that hardness rise which is related to the pressure-induced phase transformation. Behavior is consistent with a view that the nucleation of  $\epsilon$ -phase is retarded below some critical duration less than 1  $\mu$ s.
6. Iron does not respond in a systematic way to changes in rarefaction rate.
7. The difference between the response of nickel and iron to the shock-wave profile is a consequence of the difference in their crystal structure and polymorphic behavior, and response to deformation in general.
8. It seems that most dislocations are formed at the shock front, or shock front and rarefaction part of the wave.

On the other hand, twinning and phase transformation seem to depend on the pulse duration. This would be expected from kinetics considerations of the nucleation and growth of these defects.

## ACKNOWLEDGEMENTS

The authors are grateful to the National Science Foundation and to the U. S. Department of the Army. Army Research Office-Durham, for their financial support of portions of this investigation. Thanks are due to the U. S. Air Force for the provision of range facilities for shock-loading experiments at Ellsworth Air Force Base, South Dakota.

## References

1. R. N. Orava and R. H. Wittman, "Techniques for the Control and Application of Explosive Shock Waves", Proc. Vth International Conference on High Energy Rate Fabrication, Denver, Colorado, June (1975).
2. M. A. Meyers, "Discussion of Residual Strength of Shock-Loaded RMI 38644", South Dakota School of Mines and Technology, Rapid City, S.D., accepted for publication in Met. Trans.
3. A. S. Appleton and J. S. Waddington, Acta Met. 12, 956 (1964).
4. A. R. Champion and R. W. Rohde, J. Appl. Phys. 41, 2213 (1970).
5. L. E. Murr and J-Y. Huang, Mat. Sci. and Eng. 19, 115 (1975).
6. M. A. Meyers, Met. Trans., submitted for publication (1977).
7. L. E. Murr and K. P. Staudhammer, Mat. Sci. 20, 35 (1975).
8. E. T. March and D. E. Mikkola, Script Met. 10, 851 (1976).
9. G. E. Dieter, in Response of Metals to High Velocity Deformation, ed. P. G. Shewmon and V. F. Zackay, Interscience, New York, p. 409 (1961).
10. R. L. Nolder and G. Thomas, Acta Met. 12, 227 (1964).
11. L. E. Murr, H. R. Vydyanath, and J. V. Foltz, Met. Trans. 1, 3215 (1970).
12. L. F. Trueb, J. Appl. Phys. 40, 2976 (1969).
13. M. F. Rose, T. L. Berger, and M. C. Inman, Trans. TMS-AIME 239, 1998 (1967).
14. L. E. Murr and D. Kuhlmann-Wilsdorf, New Mexico Institute of Mining and Technology, Socorro, New Mexico 87801, U.S.A., submitted to Acta Met. (1977).
15. E. G. Zukas, Metals Eng. Quant. 6, 1, May (1966).
16. G. E. Dieter, in Strengthening Mechanisms in Solids, ASM, Metals Park, Ohio, p. 279 (1962).
17. K. P. Staudhammer and L. E. Murr, "Effect of Shock Stress Amplitude, Shock Stress Duration and Prior Deformation on the Residual Micro-structure of Explosively Deformed Stainless Steel", Source cited in Ref. 1.
18. M. A. Meyers, South Dakota School of Mines and Technology, Rapid City, S.D., Unpublished work (1977).

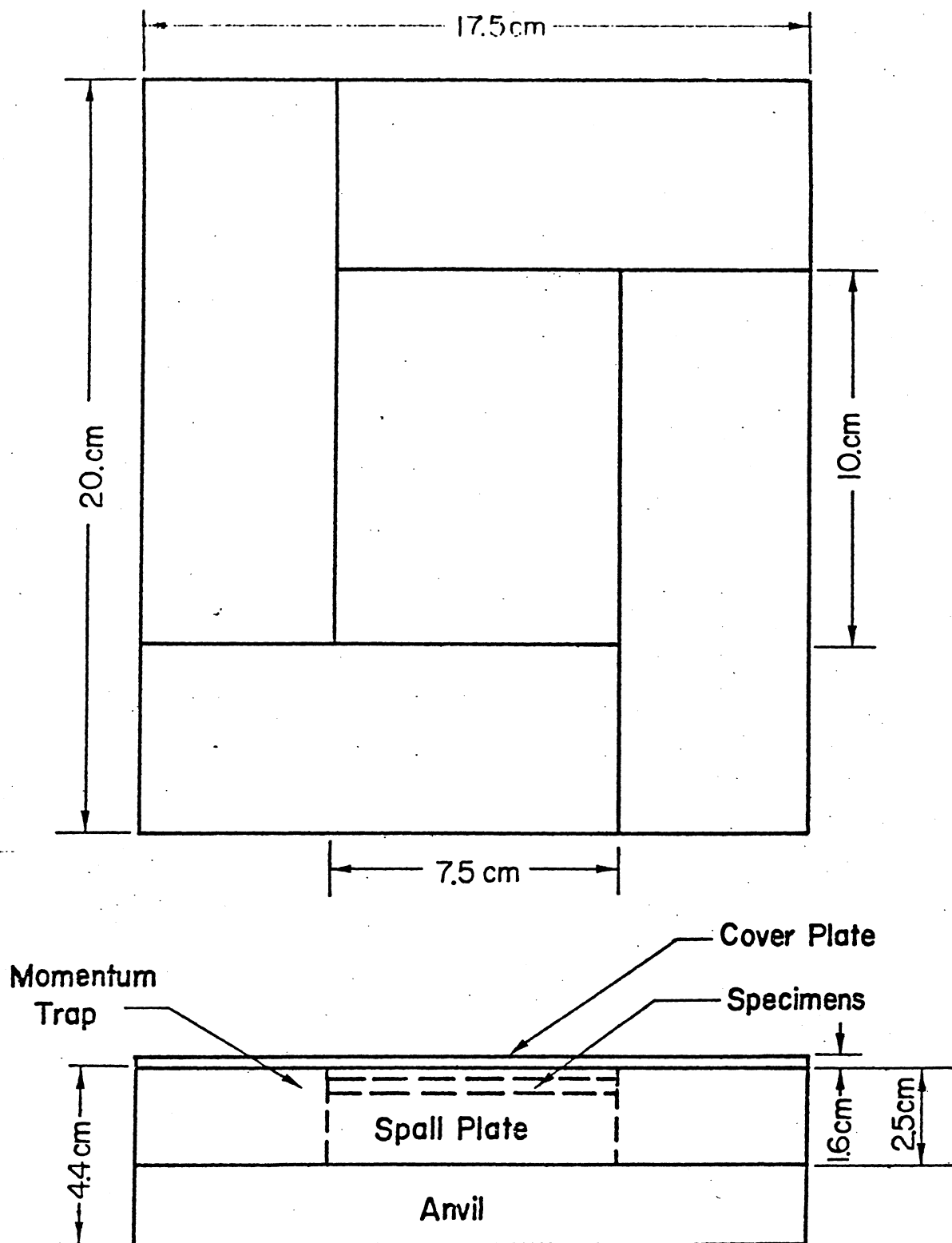


Figure 1. Specimen Assembly for Iron.

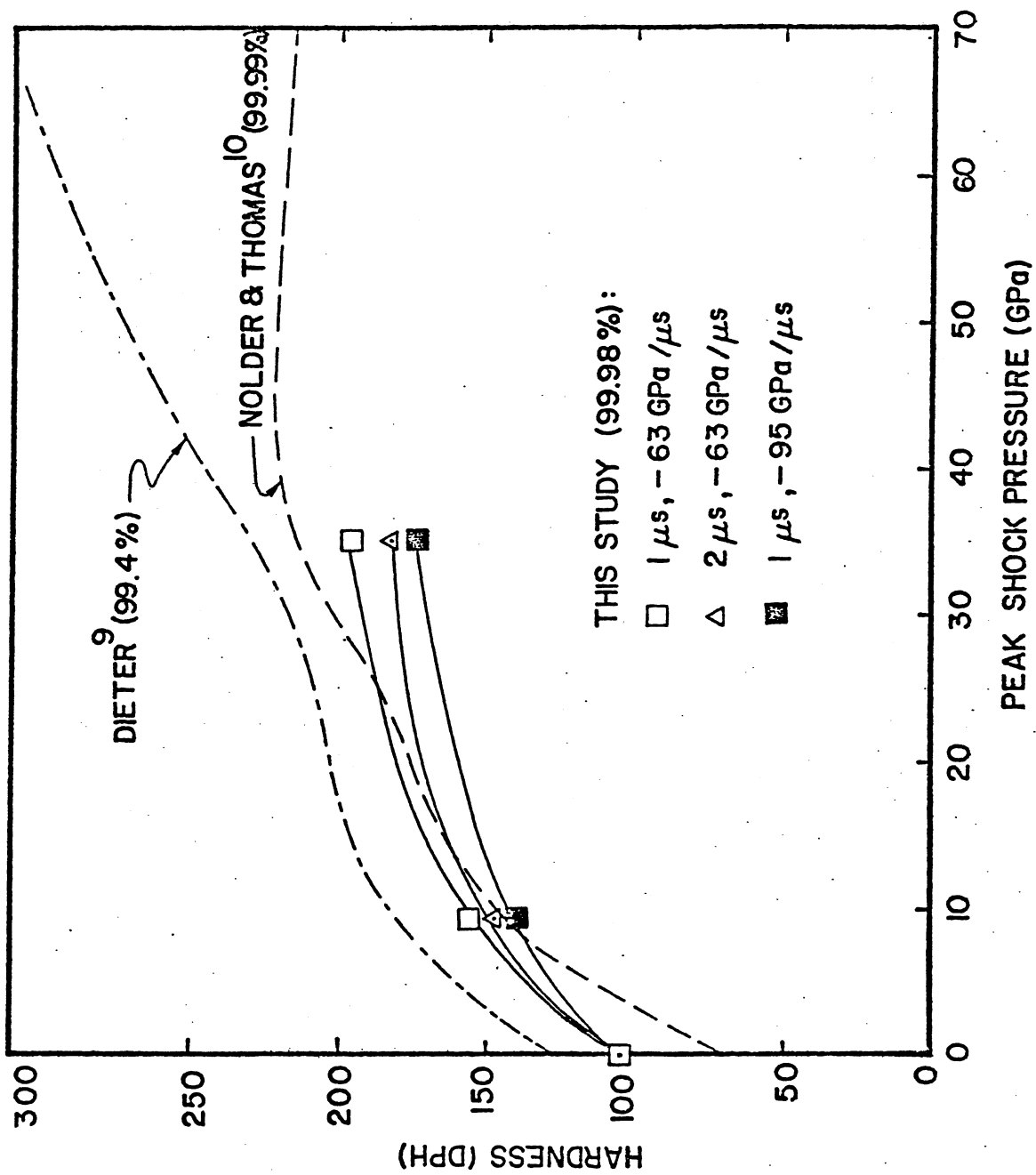
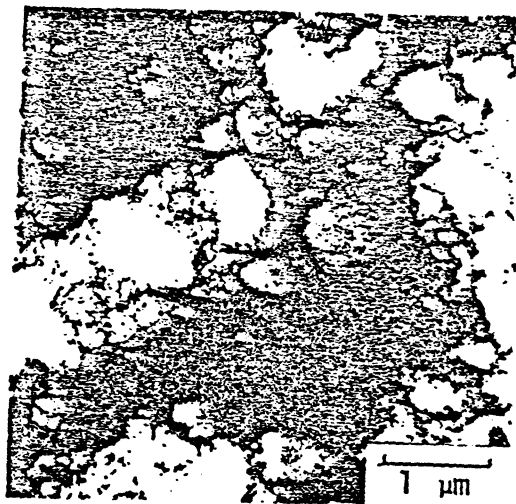
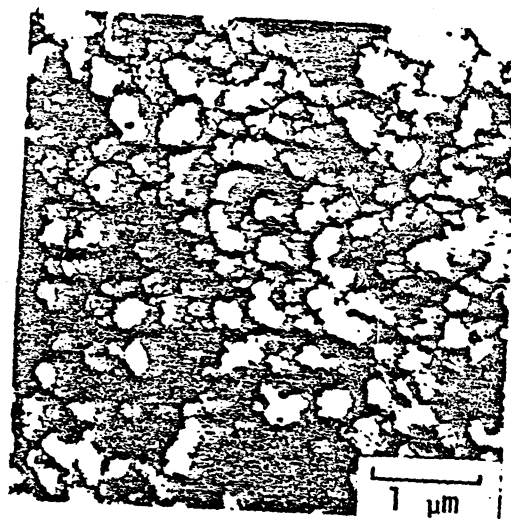


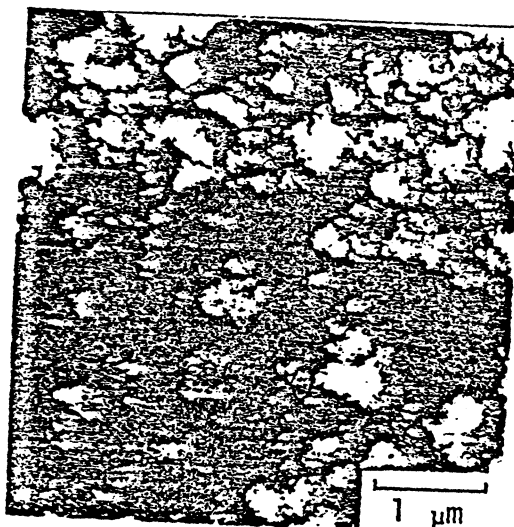
Figure 2. Shock-Hardening Curves for Nickel.



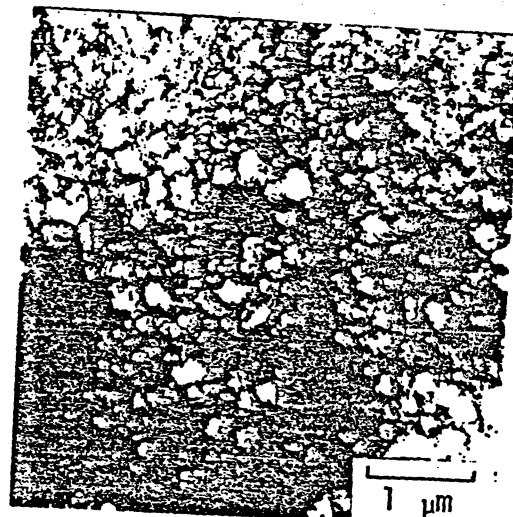
(a) 9.4 GPa, 2  $\mu$ s, -55.8 GPa/ $\mu$ s



(b) 35 GPa, 2  $\mu$ s, -69.4 GPa/ $\mu$ s



(c) 9.4 GPa, 1  $\mu$ s, -56.5 GPa/ $\mu$ s



(d) 35 GPa, 2  $\mu$ s, -38.1 GPa/ $\mu$ s

Figure 3. Transmission electron micrographs of shock-loaded Ni 270. Fail orientations close to  $\langle 110 \rangle$ .



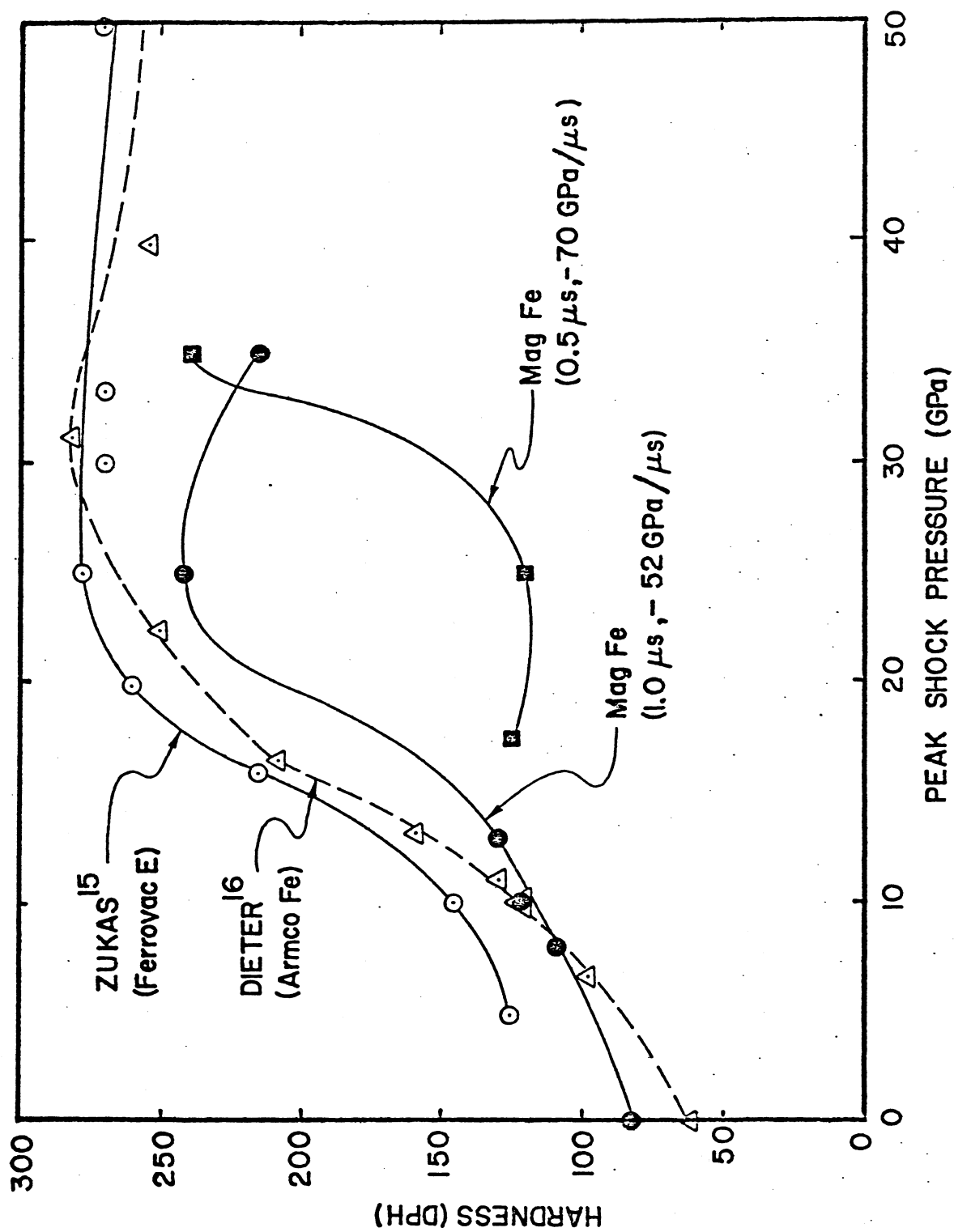


Figure 4. Shock-Hardening Curves for Iron.

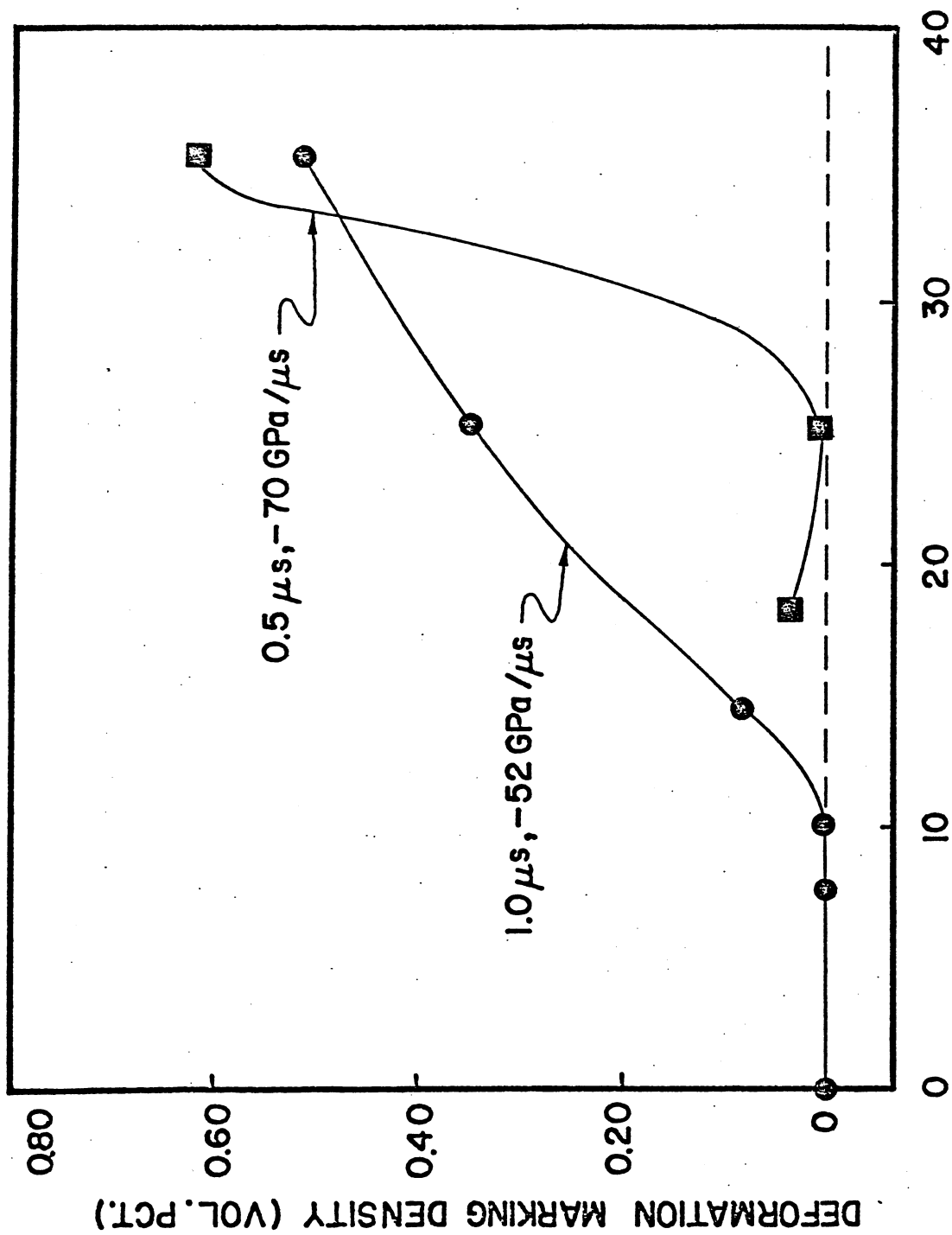
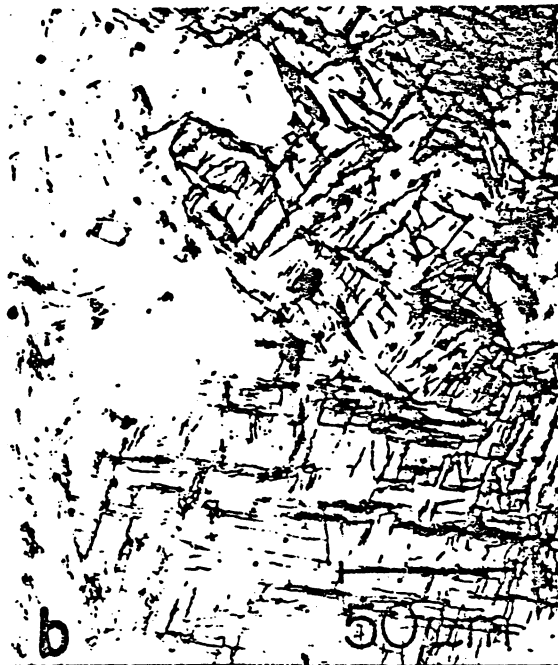


Figure 5. Shock-Pressure Dependence of Density of Deformation Markings in Magnetic Ingot Iron.



(a) 25 GPa, 0.5  $\mu$ s, -71.8 GPa/ $\mu$ s



(b) 25 GPa, 1.0  $\mu$ s, -70.5 GPa/ $\mu$ s

Figure 6. Dependence of deformation structure on pressure duration in iron. Optical.